

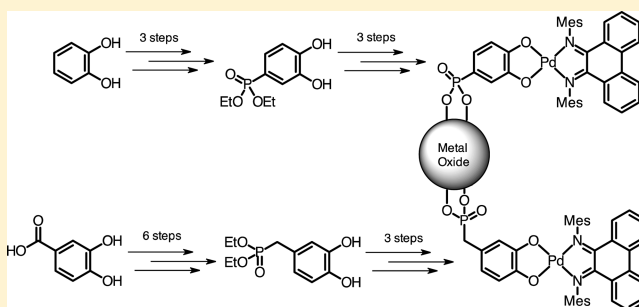
Synthesis of Catecholate Ligands with Phosphonate Anchoring Groups

Elaine Seraya,[†] Zhongyue Luan,[‡] Matt Law,^{†,‡} and Alan F. Heyduk^{*,†}[†]Department of Chemistry, University of California, Irvine, California 92697, United States[‡]Department of Chemical Engineering and Materials Science, University of California, Irvine, California 92697, United States

S Supporting Information

ABSTRACT: New catecholate ligands containing protected phosphonate anchoring groups in the 4-position of the catecholate ring were synthesized. The catechol 4-diethoxyphosphorylbenzene-1,2-diol, (^{Et}phoscat)²⁻, was prepared in three steps from pyrocatechol; whereas, the catechol 4-(diethoxyphosphorylmethyl)benzene-1,2-diol, (^{Et}Bnphoscat)²⁻, containing a methylene spacer between the catecholate ring and phosphonate anchor, was prepared from protocatechuic acid in six linear steps. Both catechol derivatives were further elaborated to their trimethylsilyl-protected counterparts to facilitate their binding to nanocrystalline metal oxides.

Electronic spectroscopy and cyclic voltammetry were used to probe the electronic properties of the phosphonate-functionalized catecholates in charge-transfer complexes of the general formula (catecholate)Pd(pdi) (pdi = *N,N'*-bis(mesityl)phenanthrene-9,10-diimine). These studies show that attachment of the phosphonate anchor directly to the 4-position of the (^{Et}phoscat)²⁻ ligand significantly perturbs the donor ability of the catecholate ligand; however, incorporation of a single methylene spacer group in (^{Et}Bnphoscat)²⁻ helps to isolate catecholate from the electron-withdrawing phosphonate group.



■ INTRODUCTION

Ligands of the *o*-dioxolene family (catecholates) once again have become prevalent in coordination chemistry. Due to the fundamental capacity of catecholate ligands to access three oxidation states when coordinated to a metal ion,¹ coordination complexes incorporating these ligands are often characterized by intriguing electronic or magnetic properties, which in turn leads to diverse potential applications. This utility of redox-active catecholates and their derivatives has expanded rapidly in recent years to include applications in electrocatalytic oxidation of water,^{2,3} and multielectron stoichiometric and catalytic C–C coupling reactions,^{4,5} heterolytic activation of H₂,^{6,7} homolytic activation of disulfides and O₂,^{8–10} dioxygenase-type chemistry,^{11,12} and the aerial oxidation of primary alcohols.¹³ Also recently, the employment of catecholato ligands was documented in the context of transition-metal catalysis tailored for hydrogenation of unsaturated hydrocarbons^{14,15} and olefin polymerization.¹⁶ Our group¹⁷ and others^{18–23} have studied catecholate–diimine and related complexes of group 10 metals as charge-transfer complexes for use in dye-sensitized solar cells.^{24–27}

Most of the above-mentioned studies involving complexes of the catecholate ligands and their derivatives have been performed in homogeneous solutions or with molecular complexes integrated into polymer matrices.^{14,15,28} In several applications, including catalysis, electrocatalysis, and dye sensitization, immobilization of catecholate coordination complexes on a solid support would be advantageous. One of

the best-established mechanisms for the immobilization of functional compounds on metal oxide surfaces is to employ a phosphonic acid linker;²⁹ however, effective methods for installing –PO₃H₂ groups onto catecholate-type ligands are limited.³⁰ To the best of our knowledge, only one such method has been reported, affording a symmetrical catechol with benzylic phosphonate groups at both the 3 and 6 positions of the catechol ring.³¹ Conversely, straightforward and scalable strategies for the installation of phosphonate anchoring groups at the more remote 4/5 positions of the catechol have not been reported.

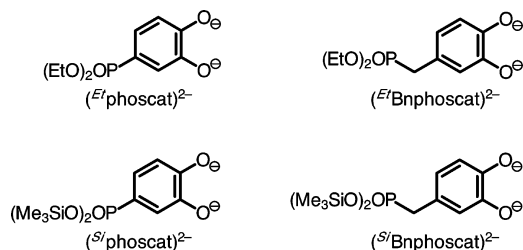
In this work, we report synthetic strategies for installing a phosphonate anchoring group at the 4-position of the catechol ring. The first derivative, 4-diethoxyphosphorylbenzene-1,2-diol, (^{Et}phoscat)²⁻, contains an ethyl-protected phosphonate group attached directly to the 4-position of the catecholate as shown in Chart 1. The second derivative, 4-(diethoxyphosphorylmethyl)benzene-1,2-diol, (^{Et}Bnphoscat)²⁻, contains a single methylene spacer unit between the ethyl-protected phosphonate group and the 4-position of the catecholate ring (Chart 1). These two derivatives required significantly different synthetic routes and were expected to confer different electronic character to the catecholate moiety. To characterize the impact that these anchoring groups have on the electronic properties of the catecholate ligands, new square-

Received: May 26, 2015

Published: July 22, 2015



Chart 1



planar palladium(II) complexes of the phosphonate-function-alized catecholates have been prepared, and their spectroscopic and electrochemical features have been measured. Finally, preliminary studies have been conducted to test the binding of these anchored-catecholate complexes to metal-oxide surfaces, which required *in situ* elaboration of $(\text{Et}^{\text{phoscat}})^{2-}$ and $(\text{Et}^{\text{Bnphoscat}})^{2-}$ to the silylated derivatives $(\text{Si}^{\text{phoscat}})^{2-}$ and $(\text{Si}^{\text{Bnphoscat}})^{2-}$, respectively, also shown in Chart 1.

EXPERIMENTAL SECTION

General Considerations. All manipulations involving the synthesis of ligands were performed under air, unless otherwise noted, employing reagents and solvents purchased from commercial suppliers and used as received. Column chromatography was performed with 230–400 mesh silica gel using flash column techniques. Palladium complexes were synthesized and studied under an inert atmosphere of nitrogen using standard glovebox techniques and dry and degassed solvents. Hydrocarbon solvents were sparged with argon and then deoxygenated and dried by passage through Q5 and activated alumina columns, respectively. Ethereal and halogenated solvents were sparged with argon and dried by passage through two activated alumina columns. Tetrachlorocatechol and 3,5-di-*tert*-butylcatechol were purchased from Sigma-Aldrich and used as received. The ligand *N,N'*-(mesityl)phenanthrene-9,10-diimine (pdi)³² and the starting material $(\text{MeCN})_2\text{PdCl}_2$ ³³ were prepared by previously described methods as were 2,2-dimethyl-1,3-benzodioxole³⁴ (**2**) and ethyl 3,4-dihydroxybenzoate (**5**).³⁵

Physical Methods. NMR spectra were collected on Bruker Avance 400 and 500 MHz spectrometers. Chemical shifts were reported using the standard δ notation in parts per million and referenced using residual ^1H and ^{13}C isotopic impurities of the solvent. Infrared spectra were recorded as KBr pellets or as neat liquids using a PerkinElmer Spectrum One FTIR spectrophotometer. Electronic absorption spectra were recorded as solutions in dry, degassed CH_2Cl_2 in 1 cm cuvettes using a PerkinElmer Lambda 900 UV–vis spectrophotometer.

Electrochemical Methods. Cyclic voltammetry (CV) and differential pulse voltammetry (DPV) experiments were performed on a Gamry series G 300 potentiostat/galvanostat/ZRA (Gamry Instruments, Warminster, PA, U.S.A.) using a 3.0 mm glassy carbon working electrode, a platinum wire auxiliary electrode, and a silver wire reference electrode. Measurements were recorded in a nitrogen-filled glovebox at ambient temperature and a scan rate of 200 mV/s. Sample concentrations were based on 1.0 mM CH_2Cl_2 solutions containing 100 mM $[\text{nBu}_4\text{N}][\text{PF}_6]$ as the supporting electrolyte. All potentials were referenced to the $[\text{Cp}_2\text{Fe}]^{+/0}$ couple using ferrocene or decamethylferrocene (-0.59 V vs $[\text{Cp}_2\text{Fe}]^{+/0}$) as an internal standard.³⁶ The typical solvent window included +2.0 V for the oxidation limit and -3.0 V for the reduction limit. Decamethylferrocene was purified by sublimation under reduced pressure and tetrabutyl-ammonium hexafluorophosphate was recrystallized from ethanol three times and dried under vacuum.

TiO₂ Binding Studies. The binding of anchor-functionalized catecholate complexes was studied using 6 μm thick films of nanocrystalline anatase TiO₂ (20 nm average particle size) on glass slides prepared according to a literature procedure.³⁷ The films were soaked in 0.5 mM solutions of the complex dissolved in methanol. To

check for binding, the films were removed from the solution and rinsed with clean solvent, and the UV–vis–NIR and FT-IR spectra were recorded. UV–vis–NIR spectra of films were recorded on a PerkinElmer Lambda 950 spectrophotometer equipped with a 60 mm integrating sphere. FT-IR spectra were recorded on a Thermo Scientific Nicolet 6700 spectrophotometer equipped with a PIKE Technologies Gladi ATR.

Diethyl (2,2-Dimethylbenzo[1,3]dioxol-5-yl)phosphonate (3a) and Diethyl (2,2-Dimethylbenzo[1,3]dioxol-4-yl)phosphonate (3b). To a solution of **2** (3.3 g, 22 mmol) and diethyl phosphite (5.7 mL, 44 mmol) in 70 mL of glacial acetic acid was added $\text{Mn}(\text{OAc})_3 \cdot \text{H}_2\text{O}$ (15 g, 56 mmol). The mixture was heated at 100 °C for 2 h while stirring in air. After cooling to room temperature, the reaction mixture was quenched with water (100 mL) and extracted with ethyl acetate (70 mL, then $2 \times 40\text{ mL}$). The combined organic layers were dried over anhydrous Na_2SO_4 and concentrated to dryness. The crude product was purified by column chromatography on silica gel (ethyl acetate/toluene, 55:45) to give an inseparable mixture of regioisomers **3a** and **3b** in a 5-to-1 ratio as an orange oil in a combined yield of 72% (4.5 g). Alternatively, the crude product may also be purified by vacuum distillation (135 °C, 0.60 mmHg). Both isomers were carried on to the next step. ^{31}P NMR (162 MHz, CDCl_3) δ 20.7; ^1H NMR (500 MHz, CDCl_3 , major) δ 7.23 (dd, $J = 14.1, 8.2\text{ Hz}$, 1H), 7.01 (d, $J = 13.2\text{ Hz}$, 1H), 6.69 (dd, $J = 7.9, 4.0\text{ Hz}$, 1H), 4.09–3.91 (m, 4H), 1.58 (s, 6H), 1.21 (t, $J = 7.4\text{ Hz}$, 6H); ^{13}C NMR (125 MHz, CDCl_3 , major) δ 151.2 (d, $J = 3.7\text{ Hz}$, aryl-C–O), 147.9 (d, $J = 22.2\text{ Hz}$, aryl-C–O), 127.1 (d, $J = 11.1\text{ Hz}$, aryl-C), 121.0 (d, $J = 193.7\text{ Hz}$, aryl-qC), 119.1 (C(CH₃)₂), 111.1 (d, $J = 12.5\text{ Hz}$, aryl-C), 108.6 (d, $J = 19.0\text{ Hz}$, aryl-C), 62.1 (d, $J = 5.5\text{ Hz}$, CH₂–O), 26.0 (CH₃), 16.4 (d, $J = 6.9\text{ Hz}$, CH₃); ^{31}P NMR (162 MHz, CDCl_3 , minor) δ 16.04. Some of the ^1H and the ^{13}C resonances of the minor regioisomer **3b** were obscured by those of the major isomer, and thus, characteristic signals are listed as follows: ^1H NMR (500 MHz, CDCl_3 , minor) δ 7.08 (dd, $J = 12.8, 7.7\text{ Hz}$, 1H), 6.77 (appar d, $J = 7.5\text{ Hz}$, 1H), 6.74 (dd, $J = 7.7, 3.7 = \text{Hz}$, 1H), 4.09–3.91 (m, 4H, minor and major), 1.61 (s, 6H), 1.24–1.20 (t, $J = 7.4\text{ Hz}$, 6H, minor and major); ^{13}C NMR (125 MHz, CDCl_3 , minor) δ 149.3 (d, $J = 3.2\text{ Hz}$, aryl-C–O), 147.7 (d, $J = 13.0\text{ Hz}$, aryl-C–O), 124.7 (d, $J = 6.9\text{ Hz}$, aryl-C), 121.2 (d, $J = 14.8\text{ Hz}$, aryl-C), 119.1 (C(CH₃)₂, minor and major), 112.3 (d, $J = 2.8\text{ Hz}$, aryl-C), 109.5 (d, $J = 190.5\text{ Hz}$, aryl-qC), 62.4 (d, $J = 5.5\text{ Hz}$, CH₂–O), 25.9 (CH₃), 16.4–16.3 (CH₃, minor and major). FTIR (neat) ν/cm^{-1} 3060, 2989, 2906, 1654, 1604, 1495 st, 1380, 1251 st, 1039 st, 963 st; HRMS (ESI) m/z calcd for $\text{C}_{13}\text{H}_{19}\text{O}_5\text{P}$ ($\text{M} + \text{Na}$)⁺ 309.0868, found 309.0869.

4-Diethoxyphosphorylbenzene-1,2-diol, (Et^{phoscat})H₂. To a solution of **3a** and **3b** (4.0 g, 14 mmol) in dry CH_2Cl_2 (200 mL) was added BCl_3 (100 mL, 1 M in hexanes) at $-78\text{ }^\circ\text{C}$ under a nitrogen atmosphere. The mixture was stirred at the same temperature for 12 h and then allowed to warm slowly to room temperature. The solvent was removed *in vacuo* to give an oily residue that was purified by silica gel column chromatography (ethyl acetate/hexanes, 40:60) to afford the product, $(\text{Et}^{\text{phoscat}})\text{H}_2$, as a single regioisomer in 67% yield (2.3 g). ^{31}P NMR (162 MHz, CDCl_3) δ 21.8; ^1H NMR (500 MHz, CDCl_3) δ 9.70 (s, 1H), 7.66 (d, $J = 15.0\text{ Hz}$, 1H), 7.13 (dd, $J = 12.6, 8.1\text{ Hz}$, 1H), 6.97–6.95 (m, 1H and s, 1H), 4.13–3.99 (4H, m), 1.30 (t, $J = 7.2\text{ Hz}$, 6H); ^{13}C NMR (125 MHz, CDCl_3) δ 149.9 (d, $J = 3.6\text{ Hz}$, aryl-C–O), 141.1 (d, $J = 21.3\text{ Hz}$, aryl-C–O), 124.6 (d, $J = 9.7\text{ Hz}$, aryl-C), 119.3 (d, $J = 3.41\text{ Hz}$, aryl-C), 117.8 (d, $J = 195.6\text{ Hz}$, aryl-qC), 115.6 (d, $J = 18.1\text{ Hz}$, aryl-C), 62.9 (d, $J = 5.1\text{ Hz}$, CH₂–O), 16.5 (d, $J = 6.5\text{ Hz}$, CH₃); FTIR (neat) ν/cm^{-1} 3521 br, 2986, 2252, 2840, 2766, 1707, 1593 st, 1511, 1423, 1283, 1009, 949, 760; HRMS (ESI) m/z calcd for $\text{C}_{10}\text{H}_{15}\text{O}_5\text{P}$ ($\text{M} + \text{Na}$)⁺ 269.0555, found 269.0553.

Ethyl 2,2-Dimethylbenzo[1,3]dioxole-5-carboxylate (6). To a stirred solution of **5** (23.4 g, 128 mmol) and acetone (56 mL) in 80 mL of benzene was added slowly phosphorus trichloride (12 mL, 137 mmol). The mixture was stirred open to air at room temperature until the evolution of HCl gas ceased, at which point the reaction flask was capped and allowed to stir for an additional 12 h. The reaction was quenched by pouring it over K_2CO_3 (75 g). The solution was filtered, and the precipitate was rinsed with benzene. Extraction with 10%

NaOH solution and drying over anhydrous Na_2SO_4 afforded product **6** in pure form as a yellow oil (18 g, 64%). While **6** is a known compound, its ^{13}C NMR data has not been reported.³⁸ ^1H NMR (500 MHz, CDCl_3) δ 7.61 (dd, J = 8.2, 1.7 Hz, 1H), 7.38 (d, J = 1.7 Hz, 1H), 6.73 (d, J = 8.2 Hz, 1H), 4.32 (q, J = 7.1 Hz, 2H), 1.69 (s, 6H), 1.36 (t, J = 7.1 Hz, 3H); ^{13}C NMR (125 MHz, CDCl_3) δ 166.5 (q, C=O), 151.7 (aryl-C-O), 147.8 (aryl-C-O), 125.1 (aryl-C), 124.2 (aryl-qC), 119.4 ($\text{C}(\text{CH}_3)_2$), 109.7 (aryl-C), 108.1 (aryl-C), 61.1 (CH_2 -O), 26.2 ($(\text{CH}_3)_2\text{C}$), 14.7 (CH_3); FTIR (neat) ν/cm^{-1} 2991, 2937, 1714 st, 1622, 1607, 1495 st, 1445 st, 1371, 1281 st, 1213 st, 1096, 1020, 980, 839, 821; HRMS (ESI) m/z calcd for $\text{C}_{12}\text{H}_{14}\text{O}_4$ ($M + \text{Na}$)⁺ 245.0790, found 245.0789.

(2,2-Dimethylbenzo[1,3]dioxol-5-yl)methanol (7). Compound **7** was prepared from 2.77 g of **6** (12 mmol) and 1.97 g of LiAlH_4 (52 mmol) in cold THF using a slightly modified literature procedure.³⁹ Standard aqueous workup afforded 2.0 g of **7** as a yellow oil (89% yield). The ^1H and ^{13}C NMR spectra of **7** are in agreement with the literature data.

5-(Bromomethyl)-2,2-dimethylbenzo[1,3]dioxole (8). To a cold (0 °C) solution of dioxole **7** (2.0 g, 11.1 mmol) and pyridine (0.95 mL, 11.6 mmol) in anhydrous Et_2O (21 mL) was added dropwise a solution of PBr_3 (0.41 mL, 4.3 mmol) in Et_2O (20 mL). The mixture was stirred for 2 h at room temperature and then quenched with ice-water (40 mL). The organic layer was separated, washed with ice-cold 1 N HCl solution (5 mL) and dried with anhydrous Na_2SO_4 . The removal of solvent by rotary evaporation yielded benzyl bromide **8** as a colorless oil (2.2 g, 81%), which was sufficiently pure to be used directly in the next step. ^1H NMR (400 MHz, CDCl_3) δ 6.81 (d, J = 7.9 Hz, 1H), 6.78 (s, 1H), 6.65 (d, J = 7.9 Hz, 2H), 4.46 (s, 2H), 1.67 (s, 6H); ^{13}C NMR (125 MHz, CDCl_3) δ 148.1 (aryl-C-O), 148.0 (aryl-C-O), 131.1 (aryl-C), 122.5 (aryl-qC), 118.8 (aryl-qC), 109.6 (aryl-C), 108.4 (aryl-C), 35.0 (CH_2 -Br), 26.2 ($(\text{CH}_3)_2\text{C}$); FTIR (neat) ν/cm^{-1} FTIR (KBr) ν/cm^{-1} 2989, 2935, 1600, 1494 st, 1448, 1257 st, 1209 st, 979, 835; HRMS (CI, positive) m/z calcd for $\text{C}_{10}\text{H}_{11}\text{BrO}_2$ (M)⁺ 241.9942, found 241.9953.

Diethyl ((2,2-Dimethylbenzo[1,3]dioxol-5-yl)methyl)phosphonate (9). A solution of benzyl bromide **8** (11 g, 45 mmol) in neat triethyl phosphite (7.8 mL, 45 mmol) was refluxed for 12 h. Upon the completion of the reaction, the obtained crude material was purified by silica gel column chromatography (EtOAc /hexanes, 42:58) to afford **9** as a yellow oil (11 g, 81%). ^{31}P NMR (162 MHz, CDCl_3 , major) δ 28.0; ^1H NMR (500 MHz, CDCl_3) δ 6.66–6.59 (m, 3H), 3.98 (apparent q, J = 7.3 Hz, 4H), 3.02 (d, J = 11.0 Hz, 2H), 1.61 (s, 6H), 1.21 (apparent t, J = 7.3 Hz, 6H); ^{13}C NMR (125 MHz, CDCl_3) δ 147.8 (d, J = 3.2 Hz, aryl-C-O), 146.7 (d, J = 3.2 Hz, aryl-C-O), 124.4 (d, J = 9.7 Hz, aryl-qC), 122.5 (d, J = 7.9 Hz, aryl-C), 118.1 ($\text{C}(\text{CH}_3)_2$), 110.4 (d, J = 6.0 Hz, aryl-C), 108.3 (d, J = 3.2 Hz, aryl-C), 62.3 (d, J = 6.9 Hz, CH_2 -O), 34.1 (d, J = 139.2 Hz, CH_2 -P), 26.0 (CH_3), 16.6 (d, J = 6.0 Hz, CH_3); FTIR (neat) ν/cm^{-1} 2988, 2911, 1650, 1609, 1498 st, 1380, 1231 st, 1048 st, 957 st 825 st; HRMS (ESI) m/z calcd for $\text{C}_{14}\text{H}_{21}\text{O}_5\text{P}$ ($M + \text{Na}$)⁺ 323.1024, found 323.1028.

4-(Diethoxyphosphorylmethyl)benzene-1,2-diol, (^{Et}Bnphoscat)H₂. To a solution of **9** (2.5 g, 8.0 mmol) in dry CH_2Cl_2 (200 mL) was added BCl_3 (20 mL, 1 M in hexanes) at -78 °C under a nitrogen atmosphere. The mixture was stirred at the same temperature for 12 h and then allowed to warm slowly to room temperature and quenched with MeOH (4 mL). The solvent was removed *in vacuo* to give an oily residue, which was purified by silica gel column chromatography (gradient MeOH/ CHCl_3 , 7:93) to afford product (^{Et}Bnphoscat)H₂ as a white solid (1.5 g, 71%). ^{31}P NMR (162 MHz, CDCl_3) δ 29.5; ^1H NMR (500 MHz, CDCl_3) δ 8.18 (s, 1H), 7.01 (s, 1H), 6.91 (s, 1H), 6.66 (d, J = 8.6, 1H), 6.55 (d, J = 8.6, 1H), 4.02 (m, 4H), 3.06 (d, J = 20.5 Hz, 2H), 1.26 (t, J = 7.2 Hz, 6H); ^{13}C NMR (125 MHz, CDCl_3) δ 145.1 (d, J = 3.2 Hz, aryl-C-O), 140.0 (d, J = 3.6 Hz, aryl-C-O), 122.0 (d, J = 9.3 Hz, aryl-qC), 121.8 (d, J = 6.94 Hz, aryl-C), 116.8 (d, J = 6.0 Hz, aryl-C), 115.6 (d, J = 3.2 Hz, aryl-C), 63.2 (d, J = 7.4 Hz, CH_2 -O), 33.6 (d, J = 140.6 Hz, CH_2 -P), 16.7 (d, J = 6.0 Hz, CH_3); FTIR (KBr) ν/cm^{-1} 3395 br, 3170 br, 2988, 1612, 1536, 1448, 1365, 1274, 1160, 1010, 860; HRMS (ESI) m/z calcd for $\text{C}_{11}\text{H}_{17}\text{O}_5\text{P}$ ($M + \text{Na}$)⁺ 283.0711, found 283.0704.

(^{Et}phoscat)Pd(pdi). A mixture of $(\text{CH}_3\text{CN})_2\text{PdCl}_2$ (127 mg, 0.500 mmol) and *N,N'*-bis(mesityl)phenanthrene-9,10-diimine (222 mg, 0.500 mmol) was stirred in CH_2Cl_2 (5 mL) at room temperature for 12 h. To the resulting dark red solution, (^{Et}phoscat)H₂ (123 mg, 0.500 mmol) was added followed by *tert*-butylamine (105 μL , 1.00 mmol). After 12 h of stirring at the same temperature, the reaction mixture was filtered to remove *tert*-butylamine hydrochloride, and the solvent was removed under vacuum. The solid residue was recrystallized from a minimum amount of dichloromethane and pentane (-35 °C) to give the product as a dark brown solid (260 mg, 66% yield). ^{31}P NMR (162 MHz, CDCl_3) δ 25.64; ^1H NMR (500 MHz, CDCl_3) δ 8.15 (d, J = 8.0 Hz, 2H), 7.62 (apparent t, J = 7.7 Hz, 2H), 7.37 (d, J = 8.3 Hz, 1H), 7.32 (d, J = 8.3 Hz, 1H), 7.12 (apparent q, J = 7.3 Hz, 2H), 7.05 (s, 4H), 6.82–6.74 (m, 2H), 6.38 (dd, J = 8.1 Hz, J = 5.0 Hz, 1H), 4.00–3.83 (m, 4H), 2.43 (s, 3H), 2.42 (s, 3H), 2.29 (s, 12H), 1.20 (t, J = 7.1 Hz, 6H); ^{13}C NMR (125 MHz, CDCl_3) δ 169.5 (d, J = 3.2 Hz, aryl-C-O), 164.7 (d, J = 20.8 Hz, aryl-C-O), 163.1 (C=N), 162.9 (C=N), 144.4 (mesityl-C-N), 144.3 (mesityl-C-N), 138.0 (mesityl-qC), 137.9 (mesityl-qC), 134.11 (pdi qC), 134.10 (pdi qC), 133.7 (pdi aryl-C), 133.6 (pdi aryl-C), 130.2 (mesityl-C), 129.69 (pdi aryl-C), 129.67 (pdi aryl-C), 129.1 (mesityl-qC), 129.0 (mesityl-qC), 128.63 (pdi aryl-C), 128.56 (pdi aryl-C), 126.6 (pdi qC), 126.5 (pdi qC), 125.12 (pdi aryl-C), 125.10 (pdi aryl-C), 122.2 (d, J = 11.1 Hz, cat aryl-C), 119.6 (d, J = 12.5 Hz, cat aryl-C), 116.4 (d, J = 19.4 Hz, cat aryl-C), 113.3 (d, J = 190.0 Hz cat aryl-qC), 61.6 (d, J = 4.6 Hz, C-O), 21.65 (mesityl-CH₃), 21.64 (mesityl-CH₃), 19.1 (mesityl-CH₃), 19.0 (mesityl-CH₃), 16.7 (d, J = 6.9 Hz, CH₃); FTIR (KBr) ν/cm^{-1} 3543, 3478, 3417, 3247, 2972, 2906, 2862, 1637, 1615, 1497, 1470, 1352, 1308 st, 1050, 1023; UV-vis-NIR (CH_2Cl_2) $\lambda_{\text{max}}/\text{nm}$ ($\epsilon/\text{M}^{-1}\text{cm}^{-1}$) 984 (8210); HRMS (ESI) m/z calcd for $\text{C}_{42}\text{H}_{43}\text{N}_2\text{O}_5\text{PPd}$ ($M + \text{Na}$)⁺ 815.1858, found 815.1871.

(^{Et}Bnphoscat)Pd(pdi). This complex was prepared in a manner similar to that described for (^{Et}phoscat)Pd(pdi) using (^{Et}Bnphoscat)H₂ (135 mg, 0.500 mmol). Recrystallization from THF and pentane (-35 °C) afforded the product as a brown solid (313 mg, 77%). ^{31}P NMR (162 MHz, CDCl_3) δ 29.5; ^1H NMR (500 MHz, CDCl_3) δ 8.16 (d, J = 8.3 Hz, 2H), 7.59 (apparent t, J = 7.3 Hz, 2H), 7.33 (d, J = 8.4 Hz, 1H), 7.30 (d, J = 8.4 Hz, 1H), 7.09 (apparent t, J = 8.3 Hz, 3.3 Hz, 2H), 7.04 (s, 4H), 6.35 (s, 1H), 6.34 (d, J = 8.0 Hz, 1H), 6.26 (d, J = 8.0 Hz, 1H), 3.94 (m, 4H), 2.96 (d, J = 20.8 Hz, 2H), 2.42 (s, 3H), 2.41 (s, 3H), 2.29 (s, 12H), 1.19 (t, J = 7.2 Hz, 6H); ^{13}C NMR (125 MHz, CDCl_3) δ 165.6 (aryl-C-O), 164.9 (aryl-C-O), 161.77 (C=N), 161.70 (C=N), 144.73 (mesityl-C-N), 144.68 (mesityl-C-N), 137.49 (mesityl-qC), 137.46 (mesityl-qC), 133.61 (pdi qC), 133.59 (pdi qC), 132.7 (pdi aryl-C), 130.00 (pdi aryl-C), 129.97 (pdi-aryl-C), 129.5 (mesityl-qC), 129.34 (pdi aryl-C), 129.31 (pdi-aryl-C), 128.0 (pdi-aryl-C), 126.8 (pdi-qC), 124.9 (pdi-aryl-C), 120.0 (d, J = 9.3 Hz, cat qC), 119.3 (d, J = 6.0 Hz, cat aryl-C), 118.1 (d, J = 6.5 Hz, cat aryl-C), 116.2 (d, J = 2.3 Hz, cat aryl-C), 62.3 (d, J = 6.9 Hz, C-O), 33.7 (d, J = 137.3 Hz, CH_2 -P), 21.6 (mesityl-CH₃), 19.08 (mesityl-CH₃), 19.07 (mesityl-CH₃), 16.7 (d, J = 6.5 Hz, CH₃); FTIR (KBr) ν/cm^{-1} 3570, 3541, 3470, 3405, 2958, 2900, 1635, 1597, 1436, 1357, 1310, 1025 st, 954; UV-vis-NIR (CH_2Cl_2) $\lambda_{\text{max}}/\text{nm}$ ($\epsilon/\text{M}^{-1}\text{cm}^{-1}$) 1298 (9360); HRMS (ESI) m/z calcd for $\text{C}_{43}\text{H}_{45}\text{N}_2\text{O}_5\text{PPd}$ ($M + \text{Na}$)⁺ 829.2015, found 829.2024.

(cat^tBu)₂Pd(pdi). This complex was prepared in a manner similar to that described for (^{Et}phoscat)Pd(pdi) using 3,5-di-*tert*-butylcatechol (111 mg, 0.500 mmol). Recrystallization from dichloromethane and pentane (-35 °C) afforded the product as a dark brown solid (360 mg, 73%). ^1H NMR (500 MHz, CDCl_3) δ 8.20 (apparent t, J = 7.5 Hz, 2H), 7.57–7.50 (m, 2H and m, 1H), 7.30 (d, J = 8.3 Hz, 1H), 7.11–7.05 (apparent quint, J = 8.0 Hz 2H), 7.04 (s, 2H), 7.00 (s, 2H), 6.42 (br s, 1H), 6.39 (s, 1H), 2.44 (s, 3H), 2.42 (d, 3H), 2.31 (s, 6H), 2.30 (s, 6H), 1.17 (s, 9H), 1.02 (s, 9H); ^{13}C NMR (125 MHz, CDCl_3) δ 167.5 (aryl-C-O), 164.0 (aryl-C-O), 159.3 (C=N), 158.6 (C=N), 145.50 (mesityl-C-N), 145.48 (mesityl-C-N), 142.8 (cat aryl-qC), 138.0 (cat aryl-qC), 136.9 (mesityl-qC), 136.8 (mesityl-qC), 132.7 (pdi qC), 132.5 (pdi qC), 131.0 (pdi aryl-C), 130.9 (pdi aryl-C), 130.3 (mesityl-qC), 129.9 (mesityl-qC), 129.8 (mesityl-C), 129.7 (mesityl-C), 128.8 (pdi aryl-C), 128.7 (pdi aryl-C), 127.24 (pdi qC), 127.20

(pdi qC), 127.1 (pdi aryl-C), 127.0 (pdi aryl-C), 124.5 (pdi aryl-C), 114.7 (cat aryl-C), 113.3 (cat aryl-C), 34.7 (C(CH₃)₃), 32.0 (cat CH₃), 29.5 (cat CH₃), 21.7 (mesityl-CH₃), 21.5 (mesityl-CH₃), 19.2 (mesityl-CH₃), 19.0 (mesityl-CH₃); FTIR (KBr) ν/cm^{-1} 3538, 3478, 3412, 3236, 2945, 2895, 2892, 1637, 1615, 1476, 1492, 1349, 1133, 1083 st, 1045, 1020; UV–vis–NIR (CH₂Cl₂) $\lambda_{\text{max}}/\text{nm}$ ($\epsilon/\text{M}^{-1}\text{cm}^{-1}$) 1414 (23620); HRMS (ESI) m/z calcd for C₄₆H₅₀N₂O₂Pd (M + Na)⁺ 791.2822, found 791.2803.

(catCl₄)Pd(pdi). This complex was prepared in a manner similar to that described for (^{Et}phoscat)Pd(pdi) using tetrachlorocatechol (124 mg, 0.500 mmol). Recrystallization from dichloromethane and pentane (–35 °C) afforded the product as a dark brown solid (312 mg, 79%). ¹H NMR (500 MHz, CDCl₃) δ 8.16 (d, *J* = 8.3 Hz, 2H), 7.66 (apparent t, *J* = 7.7 Hz, 2H), 7.51 (d, *J* = 8.3 Hz, 2H), 7.16 (apparent t, *J* = 7.7 Hz, 2H), 7.08 (s, 4H), 2.41 (s, 6H), 2.31 (s, 12H); ¹³C NMR (125 MHz, CDCl₃) δ 163.9 (C=N), 159.1 (aryl-C–O), 143.9 (mesityl-C–N), 138.5 (mesityl-qC), 134.4 (pdi aryl-C and pdi qC), 130.3 (mesityl-C), 130.0 (pdi aryl-C), 129.0 (mesityl-qC), 128.9 (pdi aryl-C), 126.3 (pdi qC), 125.2 (pdi aryl-C), 117.8 (aryl-C–Cl), 116.7 (aryl-C–Cl), 21.6 (mesityl-CH₃), 19.1 (mesityl-CH₃); FTIR (KBr) ν/cm^{-1} 3538, 3406, 3236, 2972, 2906, 1638, 1617, 1595, 1469, 1417 st, 1355, 1307, 1261 st, 1199, 1032, 972; UV–vis–NIR (CH₂Cl₂) $\lambda_{\text{max}}/\text{nm}$ ($\epsilon/\text{M}^{-1}\text{cm}^{-1}$) 932 (7400); HRMS (ESI) m/z calcd for C₃₈H₃₀Cl₄N₂O₂Pd (M + Na)⁺ 816.9985, found 816.9960.

(pdi)PdCl₂. A mixture of (CH₃CN)₂PdCl₂ (262 mg, 1.01 mmol) and *N,N'*-bis(mesityl)phenanthrene-9,10-diimine (443 mg, 1.01 mmol) was stirred in CH₂Cl₂ (10 mL) at room temperature for 18 h. The resulting dark red solution was concentrated to dryness under vacuum to afford the product as a brown solid (507 mg, 81% yield). ¹H NMR (400 MHz, CDCl₃) δ 8.07 (d, *J* = 8.2 Hz, 2H), 7.63 (apparent t, *J* = 7.4 Hz, 2H), 7.18 (d, *J* = 8.4 Hz, 2H), 7.07 (apparent t, *J* = 7.8 Hz, 2H), 7.02 (s, 4H), 2.37 (s, 6H), 2.32 (s, 12 H); ¹³C NMR (125 MHz, CDCl₃) δ 167.1 (C=N), 145.0 (mesityl-C–N), 138.3 (mesityl-qC), 135.5 (pdi aryl-C), 135.4 (pdi qC), 130.2 (mesityl-C), 130.1 (pdi aryl-C), 130.0 (mesityl-qC), 128.4 (pdi aryl-C), 126.0 (pdi qC), 125.2 (pdi aryl-C), 21.6 (mesityl-CH₃), 19.0 (mesityl-CH₃); FTIR (KBr) ν/cm^{-1} 2923, 1593, 1476, 1434, 1347, 1292, 1182, 1028, 906, 872, 725, 603; HRMS (ESI) m/z calcd for C₃₂H₃₀Cl₂N₂Pd (M + Na)⁺ 641.0725, found 641.0701.

(pdi)PdI₂. A mixture of (pdi)PdCl₂ (927 mg, 1.50 mmol) and sodium iodide (782 mg, 5.25 mmol) was vigorously stirred in CH₂Cl₂ (5 mL) at room temperature for 18 h. The resulting dark brown solution was filtered, and the filtrate was concentrated to dryness under vacuum to afford the product as a dark brown solid (2.06 mg, 91% yield). ¹H NMR (500 MHz, CDCl₃) δ 8.04 (d, *J* = 8.0 Hz, 2H), 7.62 (apparent t, *J* = 7.3 Hz, 2H), 7.31 (d, *J* = 8.5 Hz, 2 H), 7.06 (apparent t, *J* = 7.4 Hz, 2H), 7.03 (s, 4H), 2.38 (s, 6 H), 2.30 (s, 12 H); ¹³C NMR (125 MHz, CDCl₃) δ 166.6 (C=N), 147.1 (mesityl-C–N), 137.3 (mesityl-qC), 135.2 (pdi aryl-C), 134.9 (pdi qC), 129.9 (mesityl-C), 129.8 (pdi aryl-C), 129.5 (mesityl-qC), 128.2 (pdi aryl-C), 126.9 (pdi qC), 125.7 (pdi aryl-C), 21.5 (mesityl-CH₃), 19.7 (mesityl-CH₃); FTIR (KBr) ν/cm^{-1} 2906, 2851, 2226, 1592, 1441, 1345, 1304, 1249, 1167, 1034, 909, 762, 724 st; HRMS (ESI) m/z calcd for C₃₂H₃₀I₂N₂Pd (M + Na)⁺ 824.9443, found 824.9418.

(^{Si}phoscat)Pd(pdi). To a solution of (^{Et}phoscat)H₂ (148 mg, 0.60 mmol) and triethylamine (172 μL , 1.23 mmol) in Et₂O (10 mL) was added bromotrimethylsilane (162 μL , 1.23 mmol) at –78 °C, and the reaction was allowed to warm to room temperature. After stirring for 3 h at room temperature, the reaction mixture was filtered to remove triethylammonium bromide, and the solvent was removed under vacuum. The obtained yellow oil (222 mg, 0.57 mmol) was subsequently dissolved in CH₂Cl₂ (5 mL) and treated with bromotrimethylsilane (225 μL , 1.71 mmol). After stirring for 12 h at room temperature, the reaction mixture was concentrated to dryness under vacuum to remove excess bromotrimethylsilane affording a yellow residue. In a separate vial, (pdi)PdI₂ (443 mg, 0.57 mmol) and AgF (216 mg, 1.71 mmol) were combined in 10 mL of CH₂Cl₂ at ambient temperature for 12 h while protecting the sample from light to prepare (pdi)PdF₂. The yellow residue (putatively (^{Si}phoscat)-TMS₂) was then dissolved in a small aliquot of CH₂Cl₂ (3 mL) and

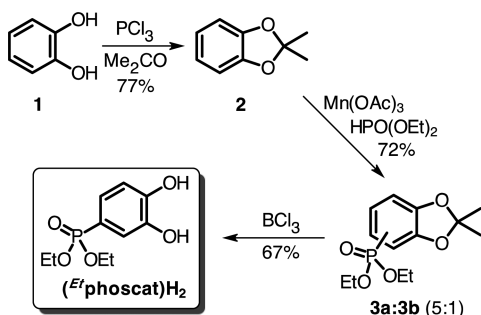
added to the solution of (pdi)PdF₂ and stirred an additional 12 h in the absence of light. The reaction mixture was filtered through a pad of Celite and concentrated to dryness under vacuum. The solid residue was recrystallized from a minimum amount of dichloromethane and pentane to give complex (^{Si}phoscat)Pd(pdi) as a brown solid (347 mg, 69% yield). ³¹P NMR (162 MHz, CDCl₃) δ 6.3; ¹H NMR (500 MHz, CDCl₃) δ 8.15 (d, *J* = 8.11 Hz, 2H), 7.62 (apparent t, *J* = 7.6 Hz, 2H), 7.40 (d, *J* = 8.5 Hz, 1H), 7.33 (d, *J* = 8.5 Hz, 1H), 7.10 (apparent q, *J* = 7.8 Hz, 2H), 7.05 (s, 4H), 6.82 (d, *J* = 15.2 Hz), 6.66 (dd, *J* = 13.6 Hz, 8.0 Hz, 1H), 6.36 (dd, *J* = 8.0 Hz, 5.0 Hz, 1H), 2.43 (s, 3H), 2.42 (s, 3H), 2.30 (s, 6H), 2.29 (s, 6H), 0.16 (s, 18H); ¹³C NMR (125 MHz, CDCl₃) δ 168.2 (d, *J* = 3.2 Hz, aryl-C–O), 164.5 (d, *J* = 21.5 Hz, aryl-C–O), 162.9 (C=N), 162.7 (C=N), 144.4 (mesityl-C–N), 144.3 (mesityl-C–N), 137.8 (mesityl-qC), 137.7 (mesityl-qC), 134.0 (pdi qC), 133.55 (pdi aryl-C), 133.52 (pdi aryl-C), 130.1 (mesityl-C), 129.6 (pdi aryl-C), 129.16 (mesityl-C), 129.12 (mesityl-C), 128.44 (pdi aryl-C), 128.36 (pdi aryl-C), 126.56 (pdi qC), 126.55 (pdi qC), 125.17 (pdi aryl-C), 125.15 (pdi aryl-C), 121.0 (d, *J* = 11.5 Hz, cat aryl-C), 119.2 (d, *J* = 12.8 Hz, cat aryl-C), 117.4 (cat aryl-qC), 116.0 (d, *J* = 20.0 Hz, cat aryl-C), 21.6 (mesityl-CH₃), 19.1 (mesityl-CH₃), 19.0 (mesityl-CH₃), 1.35 (Si-(CH₃)₃); FTIR (KBr) ν/cm^{-1} 2939, 1652, 1602, 1470, 1418, 1353, 1303, 1254, 1161, 1081, 1010, 840, 766, 716, 717, 598, 535; UV–vis–NIR (CH₂Cl₂) $\lambda_{\text{max}}/\text{nm}$ ($\epsilon/\text{M}^{-1}\text{cm}^{-1}$) 1014 (8940); HRMS (ESI) m/z calcd for C₄₄H₅₁N₂O₅PPdSi₂ (M)⁺ 880.2125, found 880.2142.

(^{Si}Bnphoscat)Pd(pdi). To a solution of (^{Et}Bnphoscat)H₂ (156 μL , 0.60 mmol) and triethylamine (172 μL , 1.23 mmol) in THF (10 mL) was added bromotrimethylsilane (162 μL , 1.23 mmol) at –78 °C, and the reaction was warmed to room temperature and stirred for 3 h. The reaction mixture was filtered to remove triethylammonium bromide, and the solvent was removed under vacuum. The obtained yellow oil (236 mg, 0.58 mmol) was subsequently dissolved in CH₂Cl₂ (5 mL) and treated with bromotrimethylsilane (230 μL , 1.74 mmol). After stirring for 12 h at room temperature, the reaction mixture was stripped to dryness to remove excess bromotrimethylsilane, after which point the yellow compound (putatively (^{Si}Bnphoscat)TMS₂) was redissolved in CH₂Cl₂ (3 mL) and added to a suspension of (pdi)PdI₂ (455 mg, 0.58 mmol) and AgF (220 mg, 1.74 mmol) in CH₂Cl₂ (10 mL) (which had been prestirred for 12 h in the absence of light). After stirring for 12 additional hours in the dark, the reaction mixture was filtered through a pad of Celite and concentrated to dryness under vacuum to afford 22 as a brown solid (349 mg, 67%). ³¹P NMR (162 MHz, CDCl₃) δ 11.2; ¹H NMR (500 MHz, CDCl₃) δ 8.16 (d, *J* = 8.15 Hz, 2 H), 7.59 (td, *J* = 7.6 Hz, 3.5 Hz, 2H), 7.38 (d, *J* = 8.5 Hz, 1H), 7.30 (d, *J* = 8.5 Hz, 1H), 7.09 (apparent q, *J* = 7.6 Hz, 2 H), 7.03 (s, 2 H), 7.00 (s, 2 H), 6.32 (d, *J* = 8.0 Hz, 1H), 6.25 (s, 1H), 6.16 (d, *J* = 8.0 Hz, 1H), 2.87 (d, *J* = 21.2 Hz, 2 H), 2.41 (s, 6 H), 2.29 (s, 6H), 2.28 (s, 6H), 0.15 (s, 18 H); ¹³C NMR (125 MHz, CDCl₃) δ 165.7 (d, *J* = 2.8 Hz, aryl-C–O), 165.0 (d, *J* = 3.0 Hz, aryl-C–O), 161.5 (C=N), 161.3 (C=N), 144.9 (mesityl-C–N), 144.7 (mesityl-C–N), 137.34 (mesityl-qC), 137.27 (mesityl-qC), 133.5 (pdi qC), 132.50 (pdi aryl-C), 132.48 (pdi aryl-C), 130.0 (mesityl-C), 129.8 (mesityl-C), 129.61 (pdi aryl-C), 129.3 (mesityl-qC), 129.2 (mesityl-qC), 127.9 (pdi aryl-C), 126.89 (pdi qC), 126.86 (pdi qC), 124.9 (pdi aryl-C), 121.8 (d, *J* = 10.5 Hz, cat qC), 119.5 (d, *J* = 7.0 Hz, cat aryl-C), 118.2 (d, *J* = 6.2 Hz, cat aryl-C), 116.2 (d, *J* = 2.4 Hz, cat aryl-C), 21.63 (mesityl-CH₃), 21.61 (mesityl-CH₃), 19.1 (mesityl-CH₃), 19.0 (mesityl-CH₃), 1.24 (Si-(CH₃)₃); FTIR (KBr) ν/cm^{-1} 2961, 2901, 1594, 1551, 1487, 1440, 1353, 1303, 1185, 1091, 842, 760, 607; UV–vis–NIR (CH₂Cl₂) $\lambda_{\text{max}}/\text{nm}$ ($\epsilon/\text{M}^{-1}\text{cm}^{-1}$) 1322 (11090); HRMS (ESI) m/z calcd for C₄₅H₅₃N₂O₅PPdSi₂ (M + 3H – 2[(CH₃)₃Si])⁺ 751.1568, found 751.1578.

RESULTS AND DISCUSSION

Synthesis. Two distinct synthetic routes, shown, were required to access the new catecholate ligands (^{Et}phoscat)H₂ and (^{Et}Bnphoscat)H₂. The (^{Et}phoscat)H₂ ligand was prepared from pyrocatechol (1) by a three-step synthesis with an overall yield of 37% as shown in Scheme 1. The route to (^{Et}phoscat)H₂

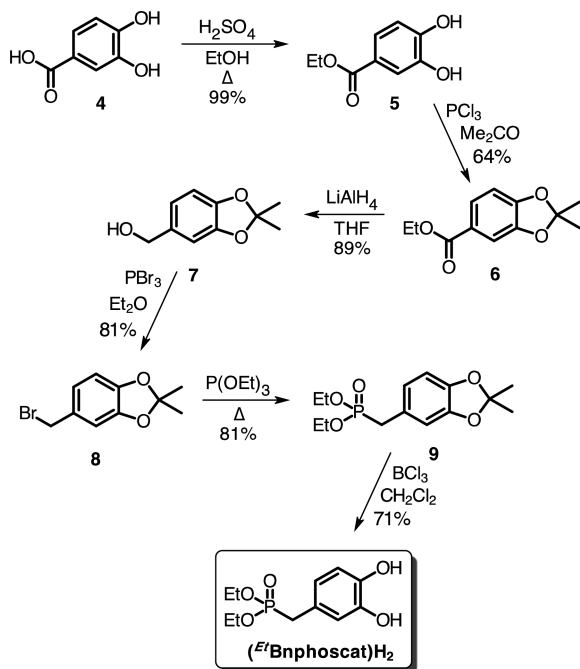
Scheme 1



proceeds via initial protection of pyrocatechol by treatment with phosphorus trichloride and acetone to afford the corresponding acetanide (2). In the next step, the phosphonate diester group was installed using diethylphosphite by a manganese(III)-promoted direct phosphorylation reaction.⁴⁰ This reaction proceeds with good regioselectivity, resulting in phosphonylation of the 4-position of the catechol ring (3a) with 5:1 selectivity over phosphonylation of the 3-position (3b, ortho to the oxygen). Attempts to separate the two isomers were not successful so both were carried through the next step. The target (^{Et}phoscat)H₂ ligand was revealed upon removal of the acetanide protecting group with boron trichloride. Purification of the unmasked catechol allowed isolation of the pure 4-phosphonylated regioisomer, 4-diethoxyphosphorylbenzene-1,2-diol, (^{Et}phoscat)H₂, by column chromatography on silica gel.

According to the procedure outlined in Scheme 2, the complementary diethyl benzylphosphonate-functionalized cat-

Scheme 2

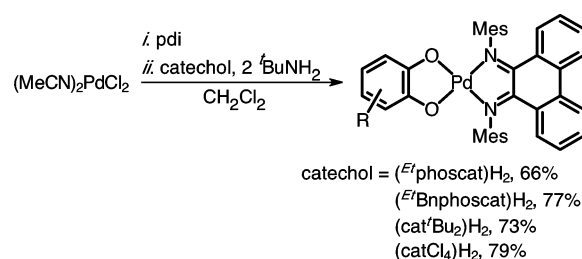


echol, (^{Et}Bnphoscat)H₂, was prepared by a six-step synthesis from protocatechuic acid (4), in an overall yield of 26% (the lowest yielding step is 64%). The route to (^{Et}Bnphoscat)H₂ commenced with esterification of protocatechuic acid followed by protection of the catechol functionality with the acetanide

using phosphorus trichloride and acetone. Reduction of the ethyl ester of 6 with lithium aluminum hydride followed by the addition of phosphorus tribromide gave benzyl bromide derivative 8. Thermolysis of the benzyl bromide derivative in neat triethylphosphite using Michaelis–Arbuzov conditions gave the ethyl-protected benzylphosphonate, 9, which was unmasked to afford (^{Et}Bnphoscat)H₂ using boron trichloride.

To benchmark the impact that phosphonate and benzylphosphonate groups have on the electronic properties of the catecholate ligand, new square-planar donor–acceptor complexes of palladium(II) were prepared. The square-planar complexes (^{Et}phoscat)Pd(pdi) and (^{Et}Bnphoscat)Pd(pdi) (pdi = *N,N'*-(mesityl)phenanthrene-9,10-diimine) were readily prepared using a one-pot, two-step reaction illustrated in Scheme 3. Addition of pdi to (MeCN)₂PdCl₂ gave (pdi)PdCl₂,

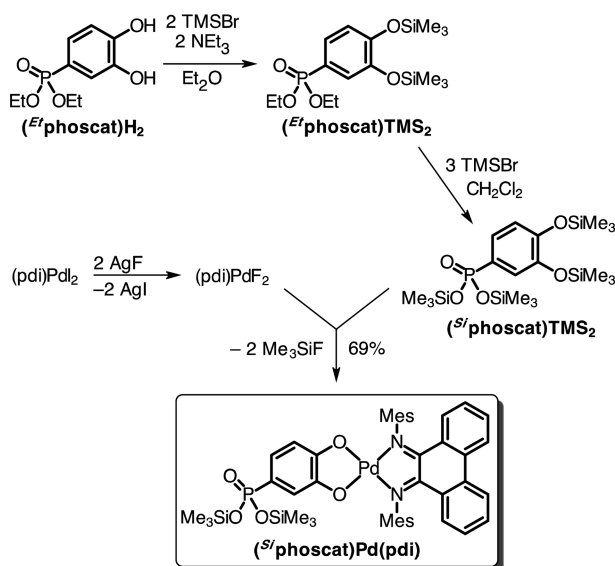
Scheme 3



which was subsequently treated with either (^{Et}phoscat)H₂ or (^{Et}Bnphoscat)H₂ in the presence of *tert*-butylamine to afford (^{Et}phoscat)Pd(pdi) or (^{Et}Bnphoscat)Pd(pdi), respectively. To better gauge the electronic properties of coordinated (^{Et}phoscat)²⁻ and (^{Et}Bnphoscat)²⁻ ligands, we prepared two additional derivatives using the procedure in Scheme 3: (cat'Bu₂)Pd(pdi) and (catCl₄)Pd(pdi) ((cat'Bu₂)²⁻ = 3,5-di-*tert*-butylcatecholate; (catCl₄)²⁻ = tetrachlorocatecholate).

The phosphonate groups of (^{Et}phoscat)²⁻ and (^{Et}Bnphoscat)²⁻ are characterized by chemically robust diethyl ester protecting groups that were expected to impede the binding of the phosphonate anchoring group to metal oxide-based surfaces. As such, silylated derivatives of both ligand platforms were sought; however, all attempts to isolate silylated ligands led to decomposition. Instead a multistep strategy was devised to generate the silylated ligand and immediately bind it to a palladium center. The conversion of the 4-(diethyl)-phosphonate substituent of (^{Et}phoscat)H₂ to a 4-bis-((trimethylsilyl)oxy)phosphonate group required the two-step silylation procedure shown in Scheme 4. Initial treatment of (^{Et}phoscat)H₂ with bromotrimethylsilane in the presence of base in diethyl ether resulted in the silylation of both *o*-dioxolenyl oxygens. The putative (^{Et}phoscat)TMS₂ derivative was not isolated and purified, but rather it was taken on to (^{Si}phoscat)TMS₂ by dealkylative silylation of the ethyl-protected phosphonate group under McKenna conditions.⁴¹ Again, putative (^{Si}phoscat)TMS₂ was not isolated, but rather it was immediately added to (pdi)PdF₂, which was generated from a mixture of (pdi)PdI₂ and AgF. The palladium fluoride synthon reacted preferentially at the catecholate site to eliminate fluorotrimethylsilane and produce (^{Si}phoscat)Pd(pdi) in 69% yield based on the initial quantity of (pdi)PdI₂. An analogous strategy was used for (^{Et}Bnphoscat)H₂ to afford (^{Si}Bnphoscat)Pd(pdi) in 67% yield.

Scheme 4



The new palladium complexes were characterized as square-planar (catecholate)Pd(diimine) complexes on the basis of their ^1H and ^{13}C NMR spectra, ESI mass spectra, electronic spectroscopies, and electrochemical data. Notably, phosphonate-containing complexes $(^{\text{Et}}\text{phoscat})\text{Pd}(\text{pdi})$ and $(^{\text{Et}}\text{Bnphoscat})\text{Pd}(\text{pdi})$ are only C_s symmetric, owing to the phosphonate anchoring group in the 4-position of the catecholate ring. This asymmetry is transferred to the pdi backbone as evidenced in both the aromatic ^1H and ^{13}C NMR resonances. In both $(^{\text{Et}}\text{phoscat})\text{Pd}(\text{pdi})$ and $(^{\text{Et}}\text{Bnphoscat})\text{Pd}(\text{pdi})$, the ^1H NMR signals of the catecholate ligand appear upfield of those for the pdi ligand, which is in accordance with the relative proton positions of the individual free ligands. In the case of coordinated $(^{\text{Et}}\text{phoscat})^{2-}$ ligand, the ^1H NMR resonances for the 3 and 5 position of the catecholate ring are shifted downfield relative to the same $(^{\text{Et}}\text{Bnphoscat})^{2-}$ resonances, which can be ascribed to the electron withdrawing nature of the phosphonate group when attached directly to the aromatic ring. The TMS-protected complexes $(^{\text{Si}}\text{phoscat})\text{Pd}(\text{pdi})$ and $(^{\text{Si}}\text{Bnphoscat})\text{Pd}(\text{pdi})$ show virtually identical ^1H and ^{13}C NMR spectral features to the ethyl-protected analogs, except the appearance of singlet resonances associated with the SiMe_3 groups and disappearance of the resonances associated with the $\text{O}-\text{CH}_2\text{CH}_3$ groups. For the palladium complexes containing the $(\text{cat}^t\text{Bu}_2)^{2-}$ and $(\text{catCl}_4)^{2-}$ ligands, the NMR spectral data is consistent with the analogous nickel complexes that have been reported previously.¹⁷

Electronic Properties of (catecholate)Pd(pdi) Complexes. The new (catecholate)Pd(pdi) complexes all display characteristic ligand-to-ligand charge-transfer (LL'CT) transitions in the UV–vis–NIR portions of the electromagnetic spectrum. Figure 1 shows the electronic absorption spectra of the six new palladium complexes measured in CH_2Cl_2 solutions at 298 K. The individual spectra reveal visibly appreciable energy differences with respect to the onset of the LL'CT absorption that track well with the relative donor capacity of the catecholate ligand. Namely, a hypsochromic shift in the lowest-energy charge-transfer band is prominent among the catecholate series in the following order: $(\text{cat}^t\text{Bu}_2)^{2-} < (^{\text{R}}\text{Bnphoscat})^{2-} < (^{\text{R}}\text{phoscat})^{2-} < (\text{catCl}_4)^{2-}$; which is generally accompanied by a sizable hypsochromic effect. As expected, the

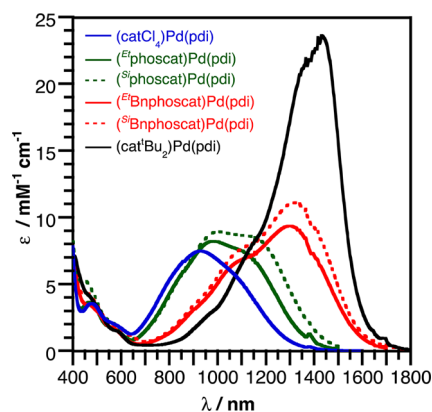


Figure 1. UV–vis–NIR absorption spectra of (catecholate)Pd-(diimine) complexes in CH_2Cl_2 at 298 K.

identity of the phosphonate protecting groups has no effect on the energy or intensity of the lowest-energy charge-transfer band, with the spectrum of $(^{\text{Et}}\text{phoscat})\text{Pd}(\text{pdi})$ being identical to that of $(^{\text{Si}}\text{phoscat})\text{Pd}(\text{pdi})$ and the spectrum of $(^{\text{Et}}\text{Bnphoscat})\text{Pd}(\text{pdi})$ being identical to that of $(^{\text{Si}}\text{Bnphoscat})\text{Pd}(\text{pdi})$. Conversely, and consistent with the NMR results, installation of the phosphonate group directly to the catecholate ring has a greater electronic impact than the installation of the phosphonate group through a methylene spacer. As such, the lowest-energy charge-transfer band of the $(^{\text{R}}\text{phoscat})\text{Pd}(\text{pdi})$ complexes is blue-shifted by approximately 800 cm^{-1} relative to the lowest-energy charge-transfer band of the $(^{\text{R}}\text{Bnphoscat})\text{Pd}(\text{pdi})$ complexes, consistent with the phosphonate group acting as an electron-withdrawing group when attached directly to the catecholate ligand.

Electrochemical analyses of the (catecholate)Pd(pdi) family of complexes further support the hypothesis that substituents on the catecholate ligand modulate the HOMO energy of the complexes. Figure 2 shows the cyclic voltammetry profiles for all six complexes recorded on CH_2Cl_2 solutions of the complex (1 mM) containing 100 mM $[\text{Bu}_4\text{N}][\text{PF}_6]$ as the supporting electrolyte; Table 1 contains the redox potentials for each complex referenced to $[\text{Cp}_2\text{Fe}]^{+/0}$ using an internal standard. In all cases, the voltammograms revealed two reversible ($i_{\text{pa}}/i_{\text{pc}} \approx$

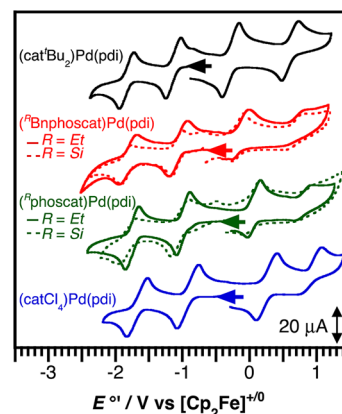


Figure 2. Cyclic voltammetry plots for (catecholate)Pd(pdi) complexes. Data acquired at 298 K on 1 mM samples dissolved in CH_2Cl_2 containing 0.1 M $[\text{Bu}_4\text{N}][\text{PF}_6]$ using a glassy-carbon electrode and a scan rate of 200 mV s^{-1} . Potentials were referenced to $[\text{Cp}_2\text{Fe}]^{+/0}$ using an internal standard.

Table 1. Electrochemical Data for (catecholate)Pd(pdi) Complexes^a

	$E_{[Pd]^{1-/2-}}^{0'}$	$E_{[Pd]^{0/1-}}^{0'}$	$E_{[Pd]^{1+/0}}^{0'}$	$E_{[Pd]^{2+/1+}}^{0'}$
(cat ^t Bu ₂)Pd(pdi)	−1.79	−1.11	−0.26	0.61
(^{Et} Bnphoscat)Pd(pdi)	−1.75	−1.03	−0.14	0.65
(^{Si} Bnphoscat)Pd(pdi)	−1.83	−1.06	−0.17	0.67
(^{Et} phoscat)Pd(pdi)	−1.72	−0.97	0.07	0.79
(^{Si} phoscat)Pd(pdi)	−1.76	−1.00	0.02	0.80
(catCl ₄)Pd(pdi)	−1.65	−0.89	0.27	0.90

^aPotentials were taken from the differential pulse voltammograms (see Supporting Information), measured at the glassy-carbon electrode in CH₂Cl₂, 0.1 M [ⁿBu₄N][PF₆] (referenced to [Cp₂Fe]^{+/0}).

1) one-electron reductions and two partially reversible oxidations ($i_{pa}/i_{pc} < 1$). Consistent with previous reports of square-planar palladium complexes bearing redox-active ligands, these redox processes can be assigned as being localized on the ligands, with the palladium center remaining in the +2 oxidation state.⁴² The reductions for all six complexes occur in narrow ranges of -1.0 ± 0.1 and -1.7 ± 0.1 V. Given that these reductions show relatively minor dependence on the identity of the catecholate ligand, they can be assigned as primarily pdi-localized reductions. The oxidative processes for all six complexes show a marked sensitivity to the identity of the catecholate ligand. An anodic shift of 530 mV is observed in the first oxidation process across the catecholate series with the potentials following the trend: (cat^tBu₂)²⁻ < (^RBnphoscat)²⁻ < (^Rphoscat)²⁻ < (catCl₄)²⁻. A similar trend was observed in the second oxidation, although the second oxidation shows relatively poor reversibility across the series. While (cat^tBu₂)-Pd(pdi) is the easiest complex to oxidize and (catCl₄)Pd(pdi) is the hardest to oxidize, the phosphonate-containing complexes fall in the middle with (^RBnphoscat)Pd(pdi) being approximately 200 mV easier to oxidize than (^Rphoscat)Pd(pdi). The observed trend is consistent with the phosphonate group acting as an electron-withdrawing group when bound to the catecholate and with the methylene spacer once again acting to insulate the catecholate from the electronic effects of the phosphonate group.

Binding of (^Rphoscat)Pd(pdi) and (^RBnphoscat)Pd(pdi) to Nanocrystalline TiO₂. Having defined the molecular structure–electronic property correlations of the phosphonate-containing catecholate ligands, we set out to examine the efficacy of both the ethyl- and silyl-protected phosphonate groups for binding to metal oxide surfaces. Given their low-cost, chemical stability, and well-established protocols for binding phosphonate-functionalized small molecules, nanocrystalline TiO₂ films were used to test both sets of (^Rphoscat)Pd(pdi) and (^RBnphoscat)Pd(pdi) complexes. Under all conditions tested, the ethyl-protected derivatives, (^{Et}phoscat)Pd(pdi) and (^{Et}Bnphoscat)Pd(pdi), failed to bind to the TiO₂ films. For these ethyl-protected derivatives, the conditions required to remove the robust ethyl groups generally cleaved the Pd–O linkage first, resulting in complete decomposition of the palladium complex as indicated by the observation of free pdi ligand by both NMR spectroscopy and mass spectrometry. In the case of the silyl-protected derivatives, (^{Si}phoscat)Pd(pdi) and (^{Si}Bnphoscat)Pd(pdi), the trimethylsilyl groups were readily hydrolyzed under the mildly protic environment provided by methanol, resulting in the binding of

the charge-transfer complex to the semiconductor surface. In a typical experiment, nanocrystalline TiO₂ films prepared on a standard silica glass slide were soaked in a 0.5 mM solution of either (^{Si}phoscat)Pd(pdi) or (^{Si}Bnphoscat)Pd(pdi), and the absorption spectrum of the film was monitored as a function of time. Within 8 h of soaking in the dye solution, strong charge-transfer absorptions were observed in the visible-to-near-IR portions of the absorption spectrum, consistent with the binding of either (^{Si}phoscat)Pd(pdi) or (^{Si}Bnphoscat)Pd(pdi) to the TiO₂ surface (see Figure S1, Supporting Information). The ready binding of the silyl-protected phosphonate-containing complexes compared with the ethyl-protected derivatives highlights the importance of choosing phosphonate protecting groups with chemistries that are compatible with the potentially reactive metal–ligand bond linkages.

CONCLUSIONS

Installation of protected phosphonate groups at the 4-position of the catecholate backbone was readily achieved using scalable synthetic strategies of modest length and overall yields. Through the synthesis of a series of palladium charge-transfer complexes, the electronic impact of directly attaching the phosphonate group to the catecholate ligand versus attaching it through a methylene linker was evaluated. Given that catecholate ligands are typically employed for their redox-activity and electron-donating ability and given that phosphonate is a significant electron-withdrawing group,⁴³ the incorporation of a single methylene linker into the (^RBnphoscat)²⁻ derivatives serves to effectively preserve the donating properties of the catecholate ligand as determined by both spectroscopic and electrochemical measurements. The phosphonate groups of both (^{Si}phoscat)²⁻ and (^{Si}Bnphoscat)²⁻ enable for robust binding to TiO₂. Furthermore, and in contrast to the previously reported di-*ortho*-phosphonylated catecholate ligand,³¹ the *para*-phosphonylated catechols described here have the anchoring group further removed from the metal-binding catecholate functionality, which should help to minimize competing interactions between the metal binding site and the metal oxide surface for immobilized dyes. As a result, the phosphonylated catecholate ligands (^Rphoscat)²⁻ and (^RBnphoscat)²⁻ reported herein should prove useful in applications such as catecholate-based dyes for sensitized solar cells or in electrochemical cells employing catecholate-based catalysts.

ASSOCIATED CONTENT

Supporting Information

¹H, ¹³C, and ³¹P NMR spectra for all new compounds and absorption spectra for palladium complexes anchored to TiO₂. The Supporting Information is available free of charge on the ACS Publications website at DOI: 10.1021/acs.inorgchem.5b01191.

AUTHOR INFORMATION

Corresponding Author

*E-mail: ahayduk@uci.edu.

Author Contributions

The manuscript was written with contributions from all authors. All authors have given approval to the final version of the manuscript.

Notes

The authors declare no competing financial interest.

ACKNOWLEDGMENTS

Financial support for this research was provided by The Research Corporation for Science Advancement Scialog: Solar Energy Conversion and the UCI Physical Sciences Center for Solar Energy. M.L. is an Alfred P. Sloan Research Fellow.

REFERENCES

- (1) Pierpont, C. G. *Coord. Chem. Rev.* **2001**, 216–217, 99–127.
- (2) Muckerman, J. T.; Polyansky, D. E.; Wada, T.; Tanaka, K.; Fujita, E. *Inorg. Chem.* **2008**, 47, 1787–1802.
- (3) Isobe, H.; Tanaka, K.; Shen, J.-R.; Yamaguchi, K. *Inorg. Chem.* **2014**, 53, 3973–3984.
- (4) Haneline, M. R.; Heyduk, A. F. *J. Am. Chem. Soc.* **2006**, 128, 8410–8411.
- (5) Smith, A. L.; Clapp, L. A.; Hardcastle, K. I.; Soper, J. D. *Polyhedron* **2010**, 29, 164–169.
- (6) Ringenberg, M. R.; Kokatam, S. L.; Heiden, Z. M.; Rauchfuss, T. B. *J. Am. Chem. Soc.* **2008**, 130, 788–789.
- (7) Deibel, N.; Schweinfurth, D.; Hohloch, S.; Fiedler, J.; Sarkar, B. *Chem. Commun.* **2012**, 48, 2388–2390.
- (8) Lippert, C. A.; Arnstein, S. A.; Sherrill, C. D.; Soper, J. D. *J. Am. Chem. Soc.* **2010**, 132, 3879–3892.
- (9) Lippert, C. A.; Riener, K.; Soper, J. D. *Eur. J. Inorg. Chem.* **2012**, 2012, 554–561.
- (10) Broere, D. L. J.; Metz, L. L.; de Bruin, B.; Reek, J. N. H.; Siegler, M. A.; van der Vlugt, J. I. *Angew. Chem., Int. Ed.* **2015**, 54, 1516–1520.
- (11) Morris, A. M.; Pierpont, C. G.; Finke, R. G. *Inorg. Chem.* **2009**, 48, 3496–3498.
- (12) Yin, C.-X.; Finke, R. G. *J. Am. Chem. Soc.* **2005**, 127, 9003–9013.
- (13) Chaudhuri, P.; Wiegardt, K.; Weyhermüller, T.; Paine, T. K.; Mukherjee, S.; Mukherjee, C. *Biol. Chem.* **2006**, 386, 1023–1033.
- (14) Camacho-Bunquin, J.; Siladke, N. A.; Zhang, G.; Niklas, J.; Poluektov, O. G.; Nguyen, S. T.; Miller, J. T.; Hock, A. S. *Organometallics* **2015**, 34, 947–952.
- (15) Kraft, S. J.; Zhang, G.; Childers, D.; Dogan, F.; Miller, J. T.; Nguyen, S. T.; Hock, A. S. *Organometallics* **2014**, 33, 2517–2522.
- (16) Kolyakina, E. V.; Poddel'sky, I.; Grishin, D. F. *Polym. Sci., Ser. B* **2014**, 56, 566–576.
- (17) Kramer, W. W.; Cameron, L. A.; Zarkesh, R. A.; Ziller, J. W.; Heyduk, A. F. *Inorg. Chem.* **2014**, 53, 8825–8837.
- (18) Pevny, F.; Zabel, M.; Winter, R. F.; Rausch, A. F.; Yersin, H.; Tuzcek, F.; Zálaiš, S. *Chem. Commun.* **2011**, 47, 6302–6304.
- (19) Heinze, K.; Reinhardt, S. *Chem. - Eur. J.* **2008**, 14, 9482–9486.
- (20) Shavaleev, N. M.; Davies, E. S.; Adams, H.; Best, J.; Weinstein, J. A. *Inorg. Chem.* **2008**, 47, 1532–1547.
- (21) Weinstein, J. A.; Tierney, M. T.; Davies, E. S.; Base, K.; Robeiro, A. A.; Grinstaff, M. W. *Inorg. Chem.* **2006**, 45, 4544–4555.
- (22) Best, J.; Sazanovich, I. V.; Adams, H.; Bennett, R. D.; Davies, E. S.; Meijer, A. J. H. M.; Towrie, M.; Tikhomirov, S. A.; Bouganov, O. V.; Ward, M. D.; Weinstein, J. A. *Inorg. Chem.* **2010**, 49, 10041–10056.
- (23) Rauth, G. K.; Pal, S.; Das, D.; Sinha, C.; Slawin, A. M. Z.; Woollins, J. D. *Polyhedron* **2001**, 20, 363–372.
- (24) Linfoot, C. L.; Richardson, P.; McCall, K. L.; Durrant, J. R.; Morandeira, A.; Robertson, N. *Sol. Energy* **2011**, 85, 1195–1203.
- (25) Geary, E. A. M.; Yellowlees, L. J.; Jack, L. A.; Oswald, I. D. H.; Parsons, S.; Hirata, N.; Durrant, J. R.; Robertson, N. *Inorg. Chem.* **2005**, 44, 242–250.
- (26) Islam, A.; Sugihara, H.; Hara, K.; Singh, L. P.; Katoh, R.; Yanagida, M.; Takahashi, Y.; Murata, S.; Arakawa, H.; Fujihashi, G. *Inorg. Chem.* **2001**, 40, 5371–5380.
- (27) Diwan, K.; Chauhan, R.; Singh, S. K.; Singh, B.; Drew, M. G. B.; Bahadur, L.; Singh, N. *New J. Chem.* **2014**, 38, 97–108.
- (28) Kraft, S. J.; Hernández Sánchez, R.; Hock, A. S. *ACS Catal.* **2013**, 3, 826–830.
- (29) Queffelec, C.; Petit, M.; Janvier, P.; Knight, D. A.; Bujoli, B. *Chem. Rev.* **2012**, 112, 3777–3807.
- (30) Saito, S.; Kawabata, J. *Helv. Chim. Acta* **2006**, 89, 1395–1406.
- (31) Honda, H.; Matsumoto, T.; Tamura, R.; Kanaizuka, K.; Kobayashi, A.; Kato, M.; Haga, M.-A.; Chang, H.-C. *Chem. Lett.* **2014**, 43, 1189–1191.
- (32) Cherkasov, V. K.; Druzhkov, N. O.; Kocherova, T. O.; Shavyrin, A. S.; Fukin, G. K. *Tetrahedron* **2012**, 68, 1422–1426.
- (33) Rimoldi, M.; Ragaini, F.; Gallo, E.; Ferretti, F.; Macchi, P.; Casati, N. *Dalton Trans.* **2012**, 41, 3648–3658.
- (34) Bikbulatov, R. R.; Timofeeva, T. V.; Zorina, L. V.; Safiev, O. G.; Zorin, V. V.; Rakhmankulov, D. L. *Russ. J. Gen. Chem.* **1996**, 66, 1805–1806.
- (35) Calderon, F. C.; García, J. L.; de la Peña, E. M.; Maya, J. M.; García, J. J. *Polym. Sci., Part A: Polym. Chem.* **2006**, 44, 2270–2281.
- (36) Connelly, N. G.; Geiger, W. E. *Chem. Rev.* **1996**, 96, 877–910.
- (37) Ito, S.; Murakami, T. N.; Comte, P.; Liska, P.; Grätzel, C.; Nazeeruddin, M. K.; Grätzel, M. *Thin Solid Films* **2008**, 516, 4613–4619.
- (38) Shigemura, R. US Patent US8148536 B2, April 3, 2012.
- (39) Kita, Y.; Arisawa, M.; Gyoten, M.; Nakajima, M.; Hamada, R.; Tohma, H.; Takada, T. *J. Org. Chem.* **1998**, 63, 6625–6633.
- (40) Xu, W.; Zou, J.-P.; Zhang, W. *Tetrahedron Lett.* **2010**, 51, 2639–2643.
- (41) McKenna, C. E.; Higa, M. T.; Cheung, N. H.; McKenna, M. C. *Tetrahedron Lett.* **1977**, 18, 155.
- (42) Kokatam, S.; Weyhermüller, T.; Bothe, E.; Chaudhuri, P.; Wiegardt, K. *Inorg. Chem.* **2005**, 44, 3709–3717.
- (43) Cheng-Ye, Y.; Wei-Zhen, X.; Meng-Juan, G.; Chi-Ying, Z. *Sci. China: Math.* **1964**, 7, 1510–1515.